



<b>Publication Year</b>	2022
<b>Acceptance in OA</b>	2025-03-07T14:49:19Z
<b>Title</b>	The telescope assembly of the Ariel space mission
<b>Authors</b>	Pace, Emanuele, TOZZI, Andrea, Abreu, Manuel Adler, Alonso, Gustavo, Barroqueiro, Bruno, Bianucci, Giovanni, Bocchieri, Andrea, BRIENZA, Daniele, BRUCALASSI, Anna, Burresti, Matteo, CANESTRARI, Rodolfo, CARBONARO, Luca, Castanheira, João., CHIOETTO, PAOLO, Colomé Ferrer, Josep, Compostizo, Carlos, CORTECCHIA, Fausto, D'ANCA, FABIO, DEL VECCHIO, Ciro, DIOLAITI, Emiliano, Eccleston, Paul, Fahmy, Salma, Fernandez Soler, Alejandro, FERRUZZI, Debora, FOCARDI, Mauro, Freitas, Sara, Galy, Camille, Garcia Perez, Andres, GOTTINI, Daniele, Grella, Samuele, Grisoni, Gabriele, GUERRIERO, Elisa, Halain, Jean-Philippe, Hellin, Marie-Laure, Ianni, Lucia, IUZZOLINO, Marcella, Jollet, Delphine, LOMBINI, Matteo, Machado, Ricardo, MALAGUTI, Giuseppe, Mazzoli, Alexandra, MICELA, Giuseppina, Miceli, Federico, Mondello, Giuseppe, MORGANTE, GIANLUCA, MUGNAI, Lorenzo, NAPONIELLO, Luca, Noce, Vladmiro, Pascale, Enzo, Perez Alvarez, Javier, PIAZZOLLA, RAFFAELE, Pompei, Carlo, Preti, Giampaolo, Roose, Stephane, Salatti, Mario, Salvignol, Jean-Christophe, Scippa, Antonio, Serre, Christophe, Simoncelli, Carlo, Teixeira, Frederico, TERENCE, Luca, Tinetti, Giovanna, Tommasi, Leonardo, Tommasi Di Vigano, Elisabetta, Vandenbussche, Bart, Vernani, Dervis, ZUPPELLA, PAOLA
<b>Publisher's version (DOI)</b>	10.1117/12.2629432
<b>Handle</b>	<a href="http://hdl.handle.net/20.500.12386/36528">http://hdl.handle.net/20.500.12386/36528</a>
<b>Serie</b>	PROCEEDINGS OF SPIE
<b>Volume</b>	12180

# The telescope assembly of the Ariel space mission

Emanuele Pace<sup>\*a,d</sup>, Andrea Tozzi<sup>d</sup>, Manuel Adler Abreu<sup>r</sup>, Gustavo Alonso<sup>o</sup>, Bruno Barroqueiro<sup>q</sup>, Giovanni Bianucci<sup>w</sup>, Andrea Bocchieri<sup>i</sup>, Daniele Brienza<sup>k</sup>, Anna Brucalassi<sup>d</sup>, Matteo Burresti<sup>u</sup>, Rodolfo Canestrari<sup>v</sup>, Luca Carbonaro<sup>d</sup>, João Castanheira<sup>q</sup>, Paolo Chioetto<sup>h,b,c</sup>, Josep Colomé Ferrer<sup>p</sup>, Carlos Compostizo<sup>s</sup>, Fausto Cortecchia<sup>e</sup>, Fabio D’Anca<sup>g</sup>, Ciro Del Vecchio<sup>d</sup>, Emiliano Diolaiti<sup>e</sup>, Paul Eccleston<sup>f</sup>, Salma Fahmy<sup>t</sup>, Alejandro Fernandez Soler<sup>o</sup>, Debora Ferruzzi<sup>d</sup>, Mauro Focardi<sup>d</sup>, Sara Freitas<sup>q</sup>, Camille Galy<sup>n</sup>, Andres Garcia Perez<sup>o</sup>, Daniele Gottini<sup>d</sup>, Samuele Grella<sup>u</sup>, Gabriele Grisoni<sup>w</sup>, Elisa Guerriero<sup>g</sup>, Jean-Philippe Halain<sup>t</sup>, Marie-Laure Hellin<sup>n</sup>, Lucia Ianni<sup>u</sup>, Marcella Iuzzolino<sup>d</sup>, Delphine Jollet<sup>t</sup>, Matteo Lombini<sup>e</sup>, Ricardo Machado<sup>q</sup>, Giuseppe Malaguti<sup>e</sup>, Alexandra Mazzoli<sup>n</sup>, Giuseppina Micela<sup>g</sup>, Federico Miceli<sup>a,d</sup>, Giuseppe Mondello<sup>u</sup>, Gianluca Morgante<sup>e</sup>, Lorenzo Mugnai<sup>i</sup>, Luca Naponiello<sup>a</sup>, Vladimiro Noce<sup>d</sup>, Enzo Pascale<sup>i</sup>, Javier Perez Alvarez<sup>o</sup>, Raffaele Piazzolla<sup>k</sup>, Carlo Pompei<sup>u</sup>, Giampaolo Preti<sup>a,d</sup>, Stephane Roose<sup>n</sup>, Mario Salatti<sup>k</sup>, Jean-Christophe Salvignol<sup>t</sup>, Antonio Scippa<sup>m</sup>, Christophe Serre<sup>p</sup>, Carlo Simoncelli<sup>u</sup>, Frederico Teixeira<sup>q</sup>, Luca Terenzi<sup>e</sup>, Giovanna Tinetti<sup>l</sup>, Leonardo Tommasi<sup>j,u</sup>, Elisabetta Tommasi Di Vigano<sup>k</sup>, Bart Vandebussche<sup>l</sup>, Dervis Vernani<sup>w</sup>, Paola Zuppella<sup>h,c</sup>

<sup>a</sup>Dip. Fisica ed Astronomia, Università di Firenze, Largo E. Fermi 2, 50125 Firenze, Italy

<sup>b</sup>Centro di Ateneo di Studi e Attività Spaziali “Giuseppe Colombo”, Via Venezia 15, 35131 Padova, Italy

<sup>c</sup>INAF-Osservatorio Astronomico di Padova, Vicolo dell’Osservatorio 5, 35122 Padova, Italy

<sup>d</sup>INAF-Osservatorio Astrofisico di Arcetri, Largo E. Fermi 5, 50125 Firenze, Italy

<sup>e</sup>INAF-Osservatorio di Astrofisica e Scienza dello Spazio di Bologna, Via Piero Gobetti 93/3, 40129 Bologna, Italy

<sup>f</sup>RAL Space, STFC Rutherford Appleton Laboratory, Didcot, Oxon, OX11 0QX, UK

<sup>g</sup>INAF-Osservatorio Astronomico di Palermo, Piazza del Parlamento 1, 90134 Palermo, Italy

<sup>h</sup>CNR-Istituto di Fotonica e Nanotecnologie di Padova, Via Trasea 7, 35131 Padova, Italy

<sup>i</sup>Dip. Fisica, La Sapienza Università di Roma, Piazzale Aldo Moro 2, 00185 Roma, Italy

<sup>j</sup>KU Leuven Instituut voor Sterrenkunde, Celestijnenlaan 200D bus 2401, 3001 Leuven, Belgium

<sup>k</sup>ASI, Agenzia Spaziale Italiana, Via del Politecnico snc, Roma, Italy

<sup>l</sup>Dept. Physics and Astronomy, University College London, Gower Street, London WC1E 6BT, UK

<sup>m</sup>Dip. Ingegneria Industriale, Università di Firenze, Via Santa Marta, 3 50139 Firenze, Italy

<sup>n</sup>Centre Spatial de Liège, Université de Liège, Avenue du Pré-Aily, B-4031 Angleur, Liège, Belgium

<sup>o</sup>Universidad Politécnica de Madrid, Plaza del Cardenal Cisneros 3, 28040 Madrid, Spain

<sup>p</sup>Institut d’Estudis Espacials de Catalunya, Gran Capità, 2-4, Edifici Nexus, Desp. 201 08034 Barcelona, Spain

<sup>q</sup>Active Space Technologies S.A., Parque Industrial de Taveiro, Lote 12, 3045-508 Coimbra, Portugal

<sup>r</sup>University of Lisbon, Institute of Astrophysics and Space Sciences, Campo Grande, Lisboa, Portugal

<sup>s</sup>Sener Aerospacial, Ctra. Campo Real, Arganda del Rey, Madrid, Spain

<sup>t</sup>ESA-ESTEC, Keplerlaan 1, 2201 AZ Noordwijk, The Netherlands

<sup>u</sup>Leonardo S.p.A., Via delle Officine Galileo 1, 50013 Campi Bisenzio, Firenze, Italy

<sup>v</sup>INAF-IASF, Via Ugo la Malfa, 153, 90146 Palermo, Italy

<sup>w</sup>Media Lario s.r.l., Via al Pascolo, 10, 23842 Bosisio Parini, Lecco, Italy

## ABSTRACT

Ariel (Atmospheric Remote-Sensing Infrared Exoplanet Large Survey) is the adopted M4 mission in the framework of the ESA “Cosmic Vision” program. Its purpose is to conduct a survey of the atmospheres of known exoplanets through transit spectroscopy. Launch is scheduled for 2029. Ariel scientific payload consists of an off-axis, unobscured Cassegrain telescope feeding a set of photometers and spectrometers in the waveband between 0.5 and 7.8  $\mu\text{m}$  and operating at cryogenic temperatures (55 K). The Telescope Assembly is based on an innovative fully-aluminum design to tolerate thermal variations avoiding impacts on the optical performance; it consists of a primary parabolic mirror with an elliptical aperture of 1.1 m of major axis, followed by a hyperbolic secondary that is mounted on a refocusing system, a parabolic re-collimating tertiary and a flat folding mirror directing the output beam parallel to the optical bench. An innovative mounting system based on 3 flexure-hinges supports the primary mirror on one side of the optical bench. The instrument bay on the other side of the optical bench houses the Ariel IR Spectrometer (AIRS) and the Fine Guidance System / NIR Spectrometer (FGS/NIRSpec). The Telescope Assembly is in phase B2 towards the Preliminary Design Review to start the fabrication of the structural model; some components, i.e., the primary mirror, its mounting system and the refocusing mechanism, are undergoing further development activities to increase their readiness level. This paper describes the design and development of the ARIEL Telescope Assembly.

**Keywords:** space telescope, Ariel mission, Infrared Telescope, cryogenic telescope, Cassegrain, aluminum mirror

## 1. INTRODUCTION

The Atmospheric Remote-sensing Infrared Exoplanet Large-survey (Ariel) mission has been adopted by ESA in November 2020 as M4 mission in the framework of the ESA 2015-2025 Cosmic Vision Program. Ariel will address the fundamental questions on what exoplanets are made of and how planetary systems form and evolve investigating the atmospheres of many hundreds of diverse planets orbiting different types of stars. Ariel will observe a large number ( $\sim 1000$ ) of warm and hot transiting gas giants, Neptunes and super-Earths around a range of host star types using differential spectroscopy in the  $\sim 1.1 - 7.8 \mu\text{m}$  spectral range and broad-band photometry in the optical and Near-IR. Generally, planets hotter than 600 K will be targeted to take advantage of their well-mixed atmospheres. Ariel is scheduled to launch in 2029.<sup>1</sup>

The Ariel Payload Module (PLM) consists of Cold Units based on an afocal, unobscured Cassegrain-type telescope<sup>2</sup> feeding a collimated beam through a Common Optics system into two separate instrument modules: the FGS<sup>3</sup>, a combined Fine Guidance System/VIS-Photometer/NIR-Spectrometer and the Ariel Infra-Red Spectrometer (AIRS)<sup>4</sup>, a 2-channel low resolution IR spectrometer. The PLM is passively cooled to  $\sim 55$  K and thermally shielded from the warm service module (SVM) by V-Groove radiators. The SVM hosts the usual spacecraft subsystems like avionics or propulsion but also the warm units of the payload, namely the Instrument Control Unit (ICU), the Detector Control Unit (DCU), the Telescope Control Unit (TCU) and FGS Control Unit (FCU) electronics.

## 2. THE TELESCOPE ASSEMBLY OVERVIEW

The Ariel Telescope Assembly (TA) consists of an all-aluminum, off-axis Cassegrain telescope, operating at cryogenic temperature ( $\sim 55$  K) and feeding a collimated beam into two separate instrument modules located on the Telescope Optical Bench (TOB) behind the Primary Mirror M1. The telescope metering structure (TMS) is fixed to the TOB on one side and supports the M2 mirror coupled to the M2 mechanism (M2M) on the other side. The TA is supported by 3 couples of Bipods and thermally shielded by 3 V-Grooves (see Fig.1).

The main characteristics of the Ariel Telescope are reported in Tab.1; its optical system is composed of four mirrors: M1 (elliptical with major axis 1.1 m x 0.7 m), M2 and M3 with a smaller diameter (respectively about 112 mm and 30 mm), and a 31 mm diameter flat folding mirror (M4). All the mirrors are made of very high-grade aluminum, an alloy that, together with the optical quality specifications, guarantees excellent thermal stability. Given the considerable size of the primary mirror, its lightening was envisaged to limit the mass. The entrance baffle, an aluminum shield surrounding the M1 mirror and the optical bench, limits the field of view of M1; an additional baffle is placed on the M2 mirror to block any direct view of the sky from M2. M2 has a refocusing mechanism with three freedom degrees (focus and tip / tilt). The aim is to correct the movements that occurred during launch and subsequent cooling and, potentially, to make occasional adjustments (for example to compensate for any long-term drifts in structural stability).

The refocusing mechanism has a heritage developed in previous ESA studies and programs: similar mechanisms have been provided for the Gaia and Euclid telescopes<sup>3,6</sup>.

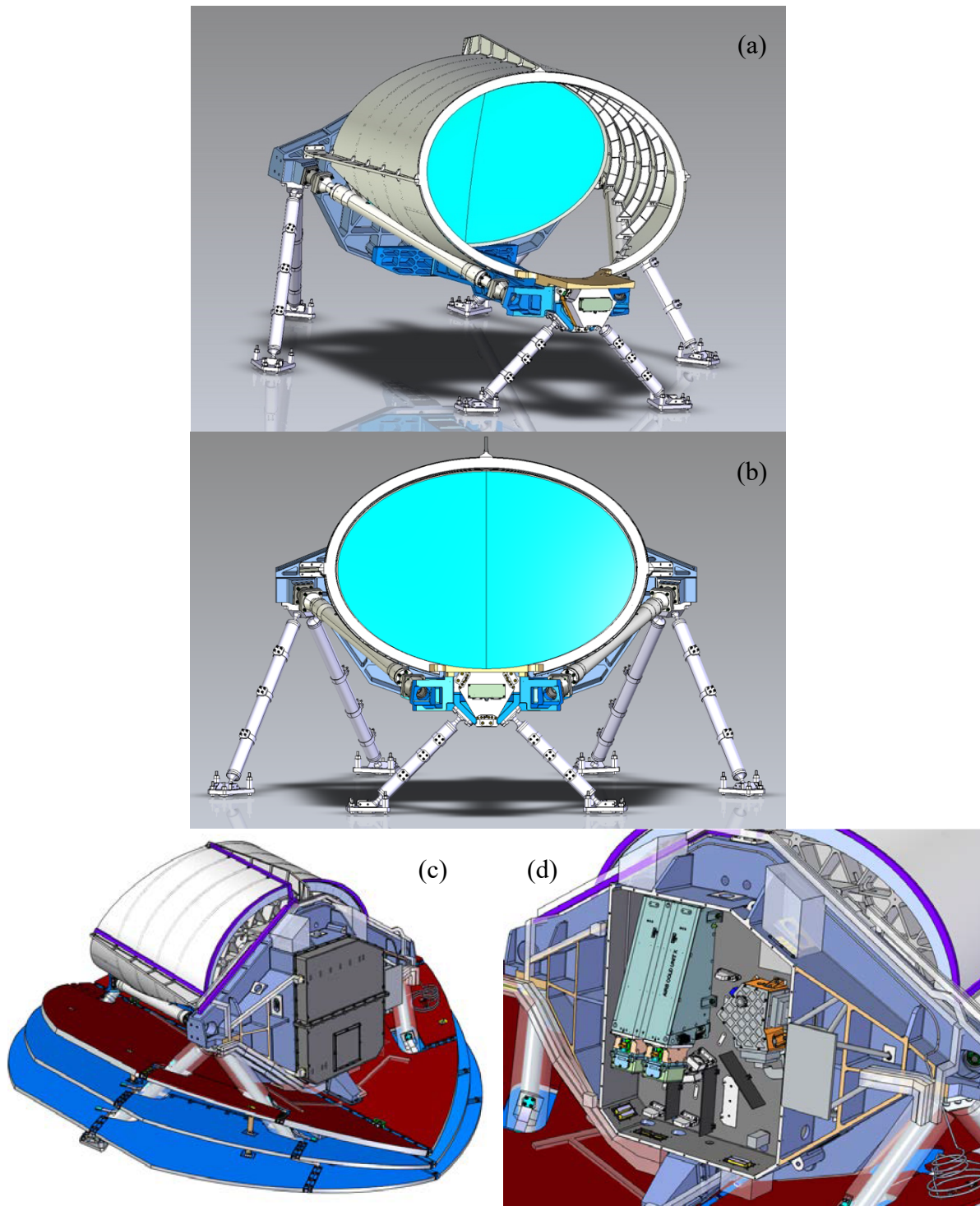


Figure 1. (a) Telescope assembly and bipods; (b) front view of the M1 mirror; (c); the Ariel payload showing the back of the telescope closed by the instrument radiator and the V-Grooves; (d) the optical bench and the instrument cavity.

The M1 mirror is supported directly by the optical bench on one side, while the two main instruments and the common optics are located on the other side. M2 and M3 mirrors are thermally decoupled from the support structures to improve the stability of the telescope; M2 is mounted on the M2 refocusing mechanism. To improve the rigidity of the telescope structure, the optical bench is provided in a position close to the midpoint of its main axis, with two aluminum alloy bars that connect OB directly to the M2 structure. The baffle is thermally and mechanically connected to the optical bench, contributing significantly to the thermal stability of the telescope. This thermo-mechanical design guarantees at the same time the necessary rigidity and excellent thermal conductivity in all directions. Hence, M4 is the optical interface of the TA to the Common Optics, while mechanical interfaces are at the bipods, the instrument radiator, the FGS and AIRS instruments, and the common optics.

Table 1. Main characteristics of the Ariel Telescope

Parameter	Value
Entrance pupil size	1100 x 730 mm
FoV	30" with diffraction limited performance 41" with optical quality TBD allowing FGS centroiding 50" unvignetted
Wavelength range	0.5 – 8 micron
WFE	Diffraction limited $\leq 3 \mu\text{m}$ (200 nm RMS)
M1 WFE	$\leq 160 \text{ nm RMS}$
M1 roughness	$< 10 \text{ nm RMS}$
M2, M3, M4 roughness	$< 2 \text{ nm RMS}$
Exit pupil (beam size)	20.4 x 13.3 mm

### 3. THE OPTICAL SYSTEM

#### 3.1 The Optical Design

The Ariel TA is an off-axis Cassegrain telescope (M1 parabola, M2 hyperbola) followed by a re-collimating off-axis parabola (M3), a plane fold mirror (M4), and the exit pupil plane. M1, M2 and M3 share a common optical axis, which lies parallel to the ARIEL X axis. Fig.2 shows the optical layout of the Ariel Telescope, while Tab.2 and Tab.3 summarize the main optical parameters of the TA mirrors.

Table 2. Main optical parameter values of the Telescope Assembly mirrors (\* @50K).

Optical element	M1	M2	M3	M4
Type	Concave mirror	Convex mirror	Concave mirror	Plane mirror
Clear aperture shape	Elliptical	Elliptical	Elliptical	Circular
Clear aperture dimensions (mm)*	1100 x 730	110 x 80	28 x 20	24
Mirror dimensions (mm)*	1125 x 771	130 x 100	50 x 45	50
R (mm)*	2319.393	239.137	511.771	Infinite
k	-1	-1.392	-1	0
Off-axis value (mm)	502	50	20	0
Surface roughness (nm RMS)	10	2	2	2
Mirror material	aluminum	aluminum	aluminum	aluminum
IR Reflective coating	Silver	Silver	Silver	Silver

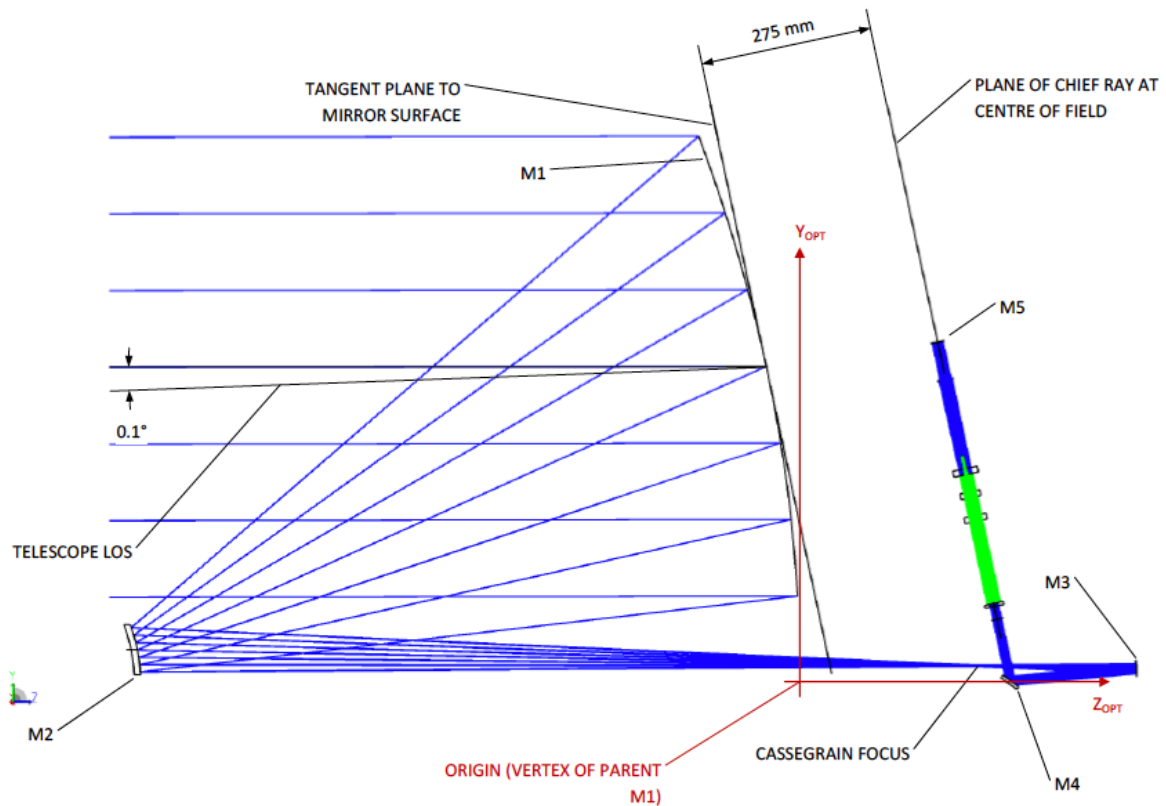


Figure 2. Scale drawing of the Ariel telescope – view in  $Y_{OPT}$ - $Z_{OPT}$  plane. The  $0.1^\circ$  offset is exaggerated for clarity.

The direction of the telescope optical axis (defined by the common M1, M2 and M3 optical axis) is parallel to the  $X_{ARIEL}$  axis. The telescope pointing axis, or line of sight (LOS), is offset by  $0.1^\circ$  with respect to the telescope optical axis to give an accessible return beam from M3.

The optical coordinate system is defined as follows:

- The origin is located at the vertex of the parent parabola for M1.
- $Z_{OPT}$  is defined as parallel to the telescope optical axis (defined by the common M1, M2 and M3 optical axis) and is positive in the direction of the incoming light.  $Z_{OPT}$  is parallel to  $X_{ARIEL}$ .
- $Y_{OPT}$  is defined as perpendicular to  $Z_{OPT}$  and to the separation plane between the LV adaptor and the s/c. It is positive in the direction going from the separation plane towards the payload.  $Y_{OPT}$  is parallel to  $Z_{ARIEL}$ .
- $X_{OPT}$  completes a right-handed set.

The  $0.1^\circ$  offset between  $Z_{OPT}$  and the telescope LOS is a rotation about  $X_{OPT}$ , in the direction shown in the system aperture stop at the M1 surface.

M4 is positioned to direct the beam onto the telescope optical bench such that all subsequent beams at the center of the field lie in a plane parallel to the tangent plane to the mirror surface. The chief ray at the center of the field is at 275 mm from the tangent plane to the mirror surface. The beam on the optical bench has its major axis parallel to the plane of the optical bench. The beam size on the optical bench is 20 mm x 13.3 mm @ operational temperature 50 K.

The telescope exit pupil aperture is reported in Tab.3; the major axis of the pupil is parallel to the plane of the optical bench. Given the optical magnification of 55 (spectral) and 54.7 (spatial), it translates to an entrance pupil at the M1 surface (system Stop) with size 1100 mm x 730 mm @ operational temperature 50K.

The design has three configurations, corresponding to the FGS and the two IR spectrometer channels. Because there are no refractive elements with any power, it is sufficient to trace a single wavelength ( $3 \mu\text{m}$  is chosen).

Table 3. Aperture limits summary

Label	Description	Aperture Decentre	Minimum Clear Aperture (half width mm)	
			30" FoV (Image quality)	50" FoV (Unvignetted)
M1 OAP	Telescope primary & aperture stop	500.0	550.0 x 365.0	
M2 HYP	Telescope secondary	49.8	52.6 x 35.3	52.6 x 35.3
Intermediate focus	Field plane between M2 & M3	24.5	1.0 x 1.0	1.7 x 1.7
M3 OAP	Collimating mirror	0	11.2 x 8.1	12.0 x 8.7
M4 PLANE	Folding mirror	0	10.4 x 10.6	10.7 x 11.0
Exit Pupil		0	10.0 x 6.7	10.0 x 6.7

### 3.2 Optical Performance

The predicted optical performances of the telescope are described, in terms of encircled energy or wavefront error or other parameter that can be useful for comparison with the scientific requirements. The analysis of the Ariel TA is dealing with an innovative type of mirror, mainly 1.1 m size M1, shaped from a monolithic slab of very high-grade aluminum; moreover, TA is required to be diffraction limited at 3  $\mu\text{m}$  and to operate as a light bucket at shorter wavelengths. For this to work, optical power needs to be concentrated in a sufficiently small and compact region of the focal planes, by ensuring suitable control of geometrical aberrations.

We have tried both to provide the correct SFE value in terms of Zernike Polynomials and to provide the methodology for measuring these errors during the machining process. Same methodology will be used to study the performance of the TA assembly during the STOP analysis.

Concerning the requirements on M1, M2, M3, and M4 mirrors, the capability of the manufacturer to perform measurements in house will be considered as a driver to fix a set of parameters that can be easily measured and evaluated during the manufacturing process.

Table 4. Encircled energy requirements at the Telescope exit pupil

Instrument name	Wavelength [micron]	Semi-major axis	semi-minor axis	semi-major axis	semi-minor axis
		83.8% Enc. Energy		91% Enc. Energy	
VISPhot	0.55	41	27	69	46
FGS1	0.7	40	26	62	41
FGS2	0.9	41	27	62	41
NIRSpec	1	42	28	62	42
	1.24	45	30	67	44
	1.48	48	32	71	47
	1.71	49	33	76	51
	1.95	53	35	83	56
AIRS CH0	1.95	53	35	83	56
	3	73	49	120	80
	3.9	91	61	152	101
AIRS CH1	3.9	91	61	152	101
	5.9	132	88	223	148
	7.8	169	113	290	193

### Encircled Energy and error budgets

The optical quality of the TA is described in terms of the radius of the encircled energy (rEE) at the TA exit pupil vs wavelength. Table 4 lists the 83.8% and 91% rEE requirements vs Ariel channels and wavelengths in units of arcsec in the collimated beam at the TA exit pupil.

Aberrations, medium frequencies, high frequency defects (e.g., surface roughness), and misalignments of the TA would impact the rEE. A detailed error budget has been estimated with the aim to provide SFE allocation for each optical surface (M1 through M4), alignment budget including launch loads, thermal deformation, vibrations, gravity error source budgets. The SFE for each mirror has been evaluated using an iterative process based on the Sensitivity Analysis of Zemax and an appropriate number of Montecarlo runs used to modify the Zernike coefficients of the mirrors' surfaces. A possible SFE allocation is shown in Figure 3 in terms of Zernike coefficients for each mirror: values are re-scaled with respect to inverse sensitivity analysis so that total SFE RMS are so distributed: M1=81 nm, M2=40 nm, M3=14 nm, M4=20 nm.

The evaluation of the error budget for the Telescope Assembly is still in progress requiring further and deeper calculations considering all the inputs and requiring iterations with the TA Industrial Prime. The co-engineering phase involving scientific team and the Prime will converge to the definition of a more accurate error budget.

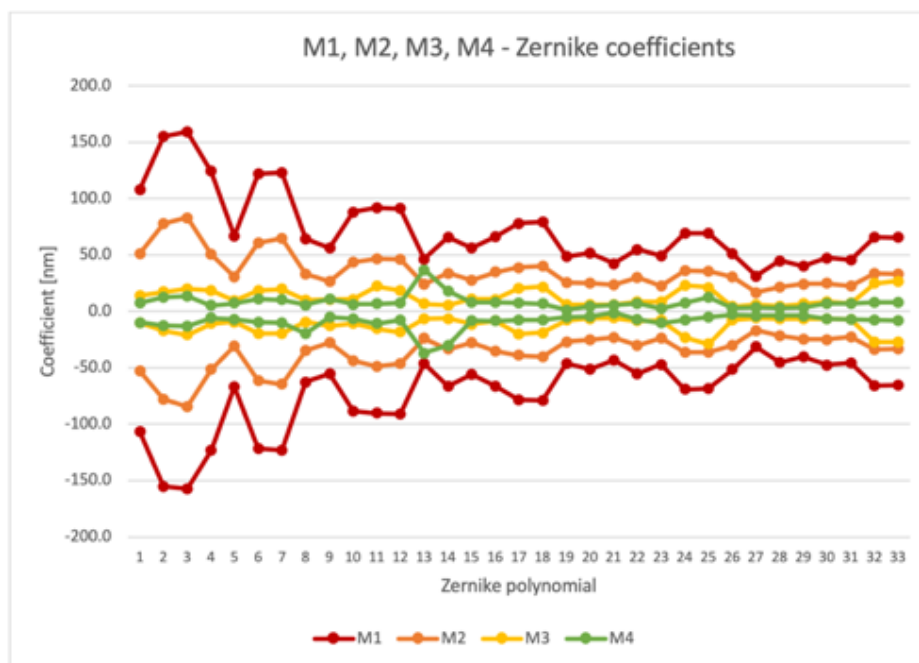


Figure 3. Zernike coefficients for each mirror having each SFE RMS equal to: M1=81 nm, M2=40 nm, M3=14 nm, M4=20 nm.

### Ag coating reflectivity

The reflectivity of the protected-Ag coating on aluminum mirror samples has been measured at CILAS, the coating manufacturer, and compared to the same coating on glass samples and to the Thorlabs values as reported in their protected-Ag coating datasheet. The measured reflectivity is shown in Fig.4. The reported values are lower than expected; some margin for improvements, especially at shorter wavelengths, are expected in the next coating development runs by optimizing the protective capping layer and surface roughness of the Al mirror as well.

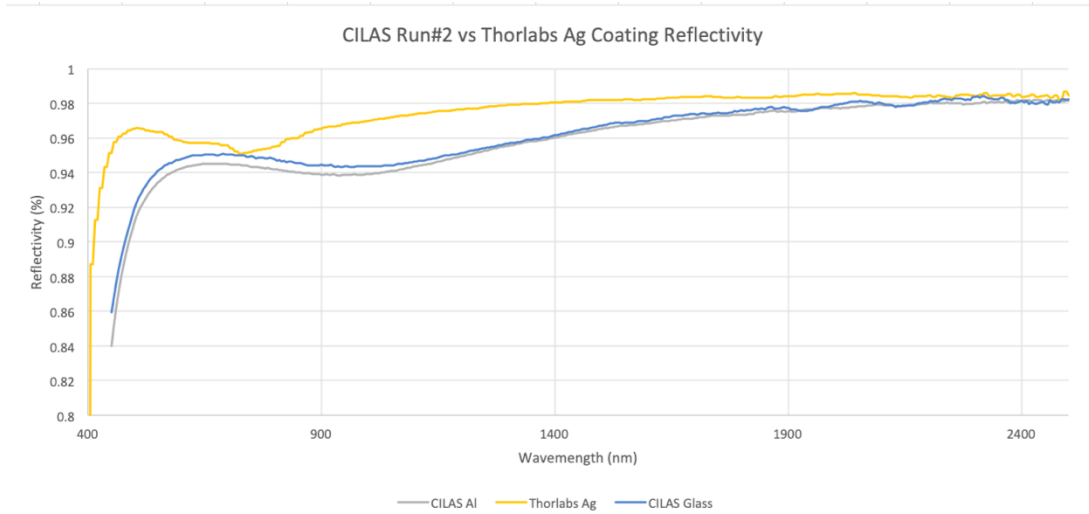


Figure 4. Protected-Ag coating measured reflectivity as compared to the expected reflectivity as reported by Thorlabs<sup>7</sup>.

### Stray Light Analysis

The first step in stray light reduction is to make the telescope as insensitive to stray light as possible. The first line of defense is the baffle at M1, which limits M1's view of the sky. The system aperture stop is located at M1, and this provides a well-defined pupil. Given that M1 is both a large surface and the first optical surface, it is likely that the out of field stray light response of the payload will be dominated by scatter from its surface. Thus, achieving sufficiently low surface roughness of the polished surface will be important.

There is a Cassegrain focus after M2 and this allows a field stop to be included in the system. This stop will be slightly oversized compared to the 50" telescope FoV (section 12.4.1.4) and will serve to attenuate both scattered light from M1 and M2 and to block any out-of-field sources close to the edge of the FoV. The field stop also serves to block any unwanted views that downstream mirrors may have of either M1 or M2.

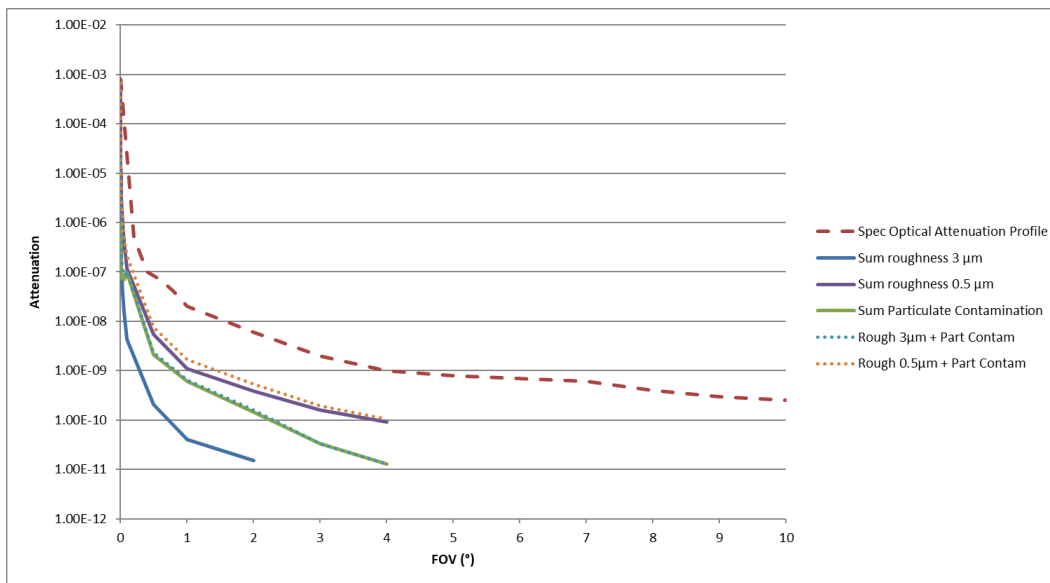


Figure 5. Mirrors micro-roughness and particulate contamination straylight for large FOV

The Ariel straylight model is defined in the ASAP<sup>®</sup> non-sequential ray-tracing software, allowing a complete parameterization of the model (optical, mechanical, thermal properties) and an easy analysis of straylight paths and levels. The complete model is made of an optical model with optical elements and properties and a mechanical model with mounts and structures for holding the optical elements as well as the telescope baffles.

Fig.5 shows the results for FOV angles as large as 4°. At that angle, the highest straylight level (corresponding to the straylight from the mirrors micro-roughness at 0.5 μm) is lower than the smallest spec value. From the curves' tendency, the straylight levels will continue to decrease with the FOV. The estimation of the final optical attenuation of the baffle B1 as a function of the FOV shows that it is several orders of magnitude lower than the specification. Being the baffle open in the lower part, stray light can be introduced in the TA because of specular reflection or scattered light from the V-Grooves. The analysis shows that the contribution to the stray light at the exit pupil is smaller than  $4.7 \times 10^{-13}$ . The same or even smaller level of stray light is introduced by the other mechanical parts of the TA.

The conclusion of the overall analysis is that no troublesome source of straylight regarding the telescope straylight specifications has been identified during the present analysis.

## 4. THE MECHANICAL DESIGN

### 4.1 Overview

The main components of the TA relevant for the mechanical design are:

- Telescope Optical Bench
- Telescope Metering Structure
- Primary mirror M1 with its mounting system
- Secondary mirror M2 supported by an M2 refocusing mechanism (M2M)
- M3, M4 mirrors
- Baffle system

All the structural elements and the telescope mirrors are made of very high-grade aluminum to provide scalable mechanical properties at the different temperatures experienced by the telescope. To increase the rigidity of the structure, the optical bench and the bipods legs have been optimised in position, angle, and thickness. The optical bench stiffness has been enhanced by including the instrument box and adding stiffening ribs.

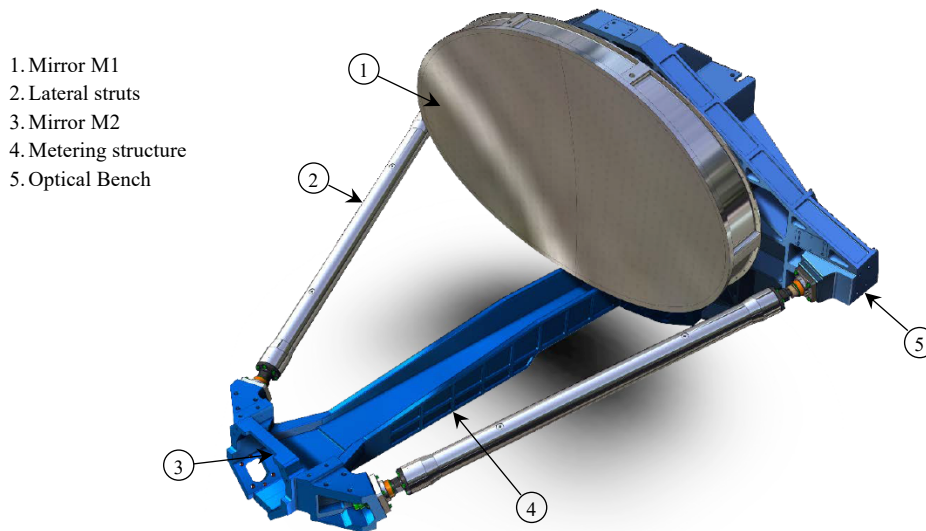


Figure 6. Mechanical assembly of the Ariel Telescope

The structure has been reinforced by the insertion of lateral struts as shown in Fig.6. These stiffening arms guarantee small deformations and high bending stiffness between M1 and M2 during application of the in-plane and out-of-plane loads. The baffle surface is mechanically and thermally connected to the TOB. This thermo-mechanical design can guarantee at the same time rigidity and a very good thermal conductance.

The key components of the TA are hereafter discussed. However, work is in progress during the phase B2 to improve the design of M1 and its mounting, the TOB thermo-mechanical coupling with M1 and baffle B1, the B1 baffle and the overall mechanical design to improve matching with the TA and Payload requirements.

#### 4.2 Telescope Optical Bench and Metering Structure

A mass saving and optimisation activity on the optical bench and the metering structure has been performed. This has cleaned up most of the features, which had evolved over the life of the project. In addition, the number of stiffeners on the front surface has been significantly reduced. Thickness of the central plane and stiffening ribs have also been revised to minimise mass. The design is still evolving in detail. The unit shown in Fig.7 is the TOB.

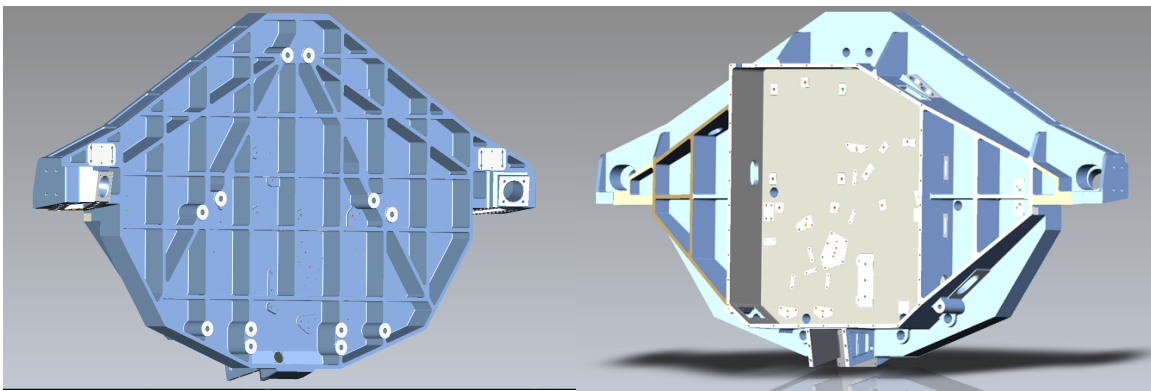


Figure 7. The Telescope Optical Bench. The mechanical, optical, and electrical interfaces are clearly shown.

This component is key to the whole of the Ariel Payload. It has critical interfaces on both surfaces. The instrument cavity (Fig.7 right panel) needs to provide a stable mechanical and thermal environment for the instruments, and on the front surface the critical interface to the M1 mounting system through 6 fixing bolts (in the upper part of the left panel in Fig.7; the lower bolts are for fixing the TMS).

All components are manufactured from the same grade of aluminium to ensure uniform thermo-mechanical behaviour of the whole assembly. This is a key issue for the design of the telescope and has been addressed within the STOP analysis of the telescope sub-system.

The TOB is directly supported on the two large rear bipods (not part of the TA), which utilise titanium flexures.

At this time the telescope optical bench is to be manufactured using conventional machining techniques using a single piece of aluminium. This is to ensure that there are no thermal discontinuities of joints and to minimise manufacturing risk. The optical bench thickness has been increased to include the instrument box as part of the structure by means of stiffening ribs on the front and rear surface. This H section gives at the bench a high structural rigidity to out-of-plane load (high mass of objects). The beam that runs from the TOB to the M2M position is the TMS. This is also connected by 2 lateral struts to the TOB to improve the mechanical rigidity.

#### 4.3 M1 mounting system

The M1 mounting based on flexure hinges is rigid to the TOB and provides the required level of isostatic mounting to minimise distortions induced in the mirror. Mounting needs to minimise mirror stresses but still ensures sufficient rigidity and strength to withstand the launch environment. The hinges' design has been selected after a detailed comparative study including the whiffle-tree design, standard hexapods, blade flexures, and flexure hinges to solve a number of mechanical and thermal constraints as very limited volume for any kind of mounting and mass budget. The mounting design based on flexures looks the most promising. Therefore, a development activity is in progress to increase the readiness of M1 and its mounting system.

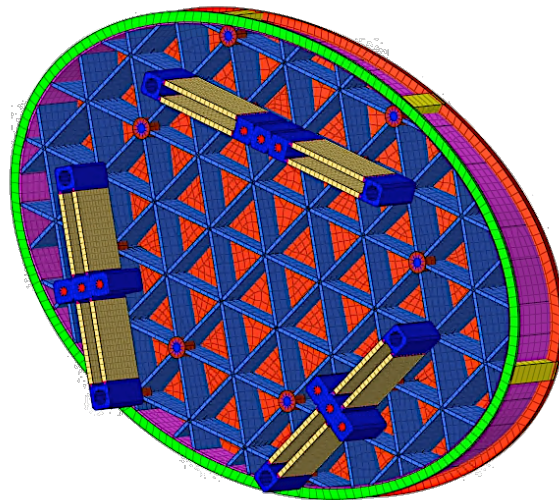


Figure 8. M1 lightweighting pattern and the mounting system based on flexure hinges

The current mechanical analysis is considering M1 with the lightweighting pattern shown in Fig.8 coupled to the TOB through the flexure hinges.

#### 4.4 Mirrors

The Ariel Telescope primary and secondary mirrors M1 and M2 are arranged in an off-axis Cassegrain configuration with M1 that is supported by the TOB as previously discussed, and M2 at the end of the TMS, as shown in Fig.6.

Also, M2 and M3 are thermally decoupled from the supporting structures for stability purposes. The M2 is mounted on the TMS: an Aluminium arm rigidly connected to the TOB that is provided at the other end with a refocus mechanism (M2M). The TMS is supported, on M2 side, by the central bipod of the Ariel PLM. M3 and M4 are arranged on a common support at the end of the TMS and under the TOB.

The mirrors will be manufactured from the same very high-grade aluminium substrate, and each will have a protected silver coating on the optical surface to improve the reflectivity in the Ariel spectral range. M1 will be lightened by > 30% to reduce the mass. The lightweighting level has been designed as the best trade-off between reducing the mass and keeping the optical surface quality in the SFE requirements.

## 5. THE THERMAL DESIGN

### 5.1 Overview

The spacecraft thermal design is based on a cold Payload Module sitting on the top of a warm Service Module. The upper surface of the Service Module has an estimated average temperature ranging between 233 K (hereafter defined as Cold Case) and 293K (hereafter defined as Hot Case). The TA, enclosed in the cold environment established by the last V-Groove, acts as an extra passive stage using its large Baffle and Optical Bench as radiating surfaces. These radiators, coated by a high IR emissivity painting, greatly improve the efficiency and the performance of the whole Payload Module passive cooling. The whole telescope structure and the mirrors achieve, at steady state, temperatures around 55 K in the Hot Case. Six main thermal interfaces can be identified between the TA and the rest of the payload (excluding the units on the TOB):

- four conductive interfaces with the head of the bipods. These 4 interfaces are expected to operate in the 58 – 63 K range and, in the Hot Case, can inject into the TA a heat leak of 36 mW per rear bipod and 69 mW for each front bipod.
- an extra conductive leak is injected by the cryo-harness. At present, this heat flux is estimated in the Hot Case to be around 150 mW at max thanks to the parasitic interception of the V-Groove stages.
- a radiative environment defined by the last V-Groove (VG3, around 62 K in the Hot Case) and the deep space (3 K). The irradiated total heat leak from VG3 to the TA is on the order of 180 mW in the Hot Case.

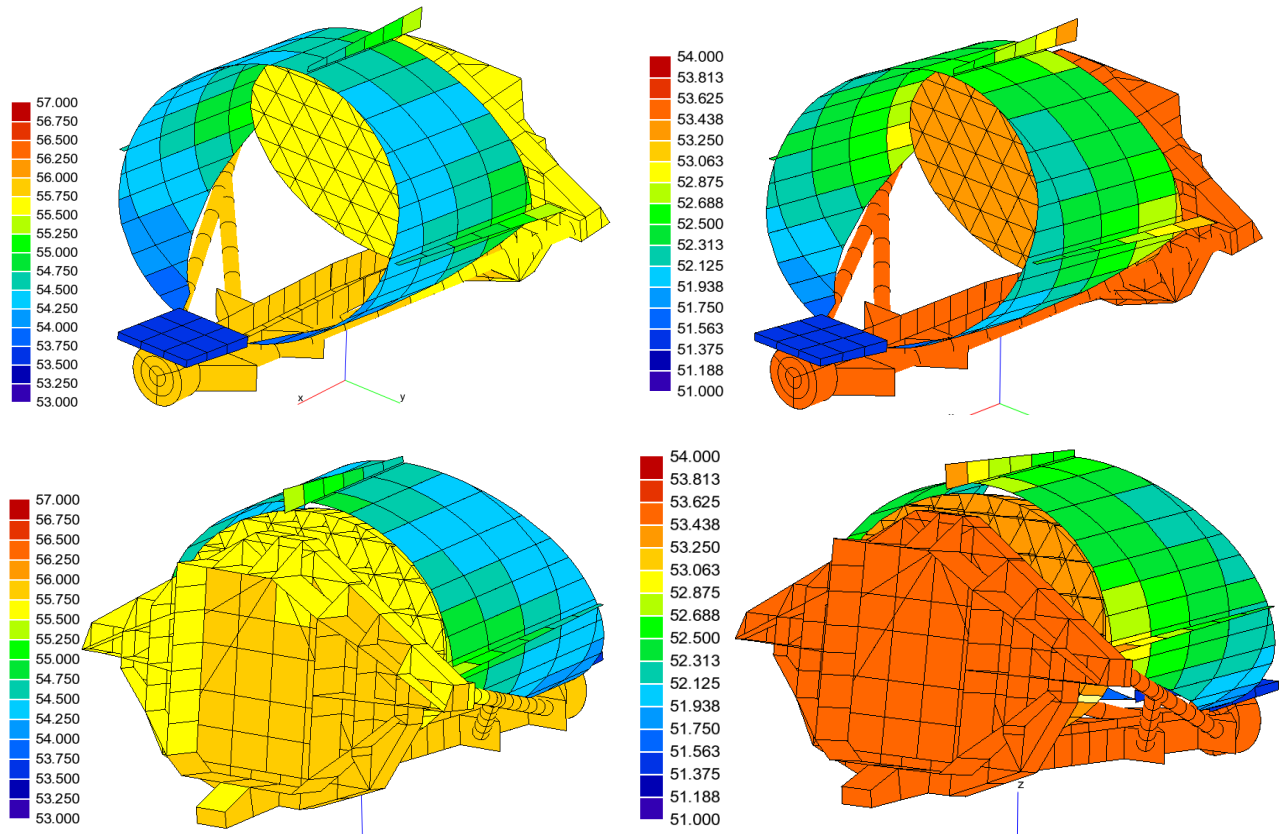


Figure 9. Views of the Telescope Assembly GTMM T map: Cold Case (right) and Hot Case (left).

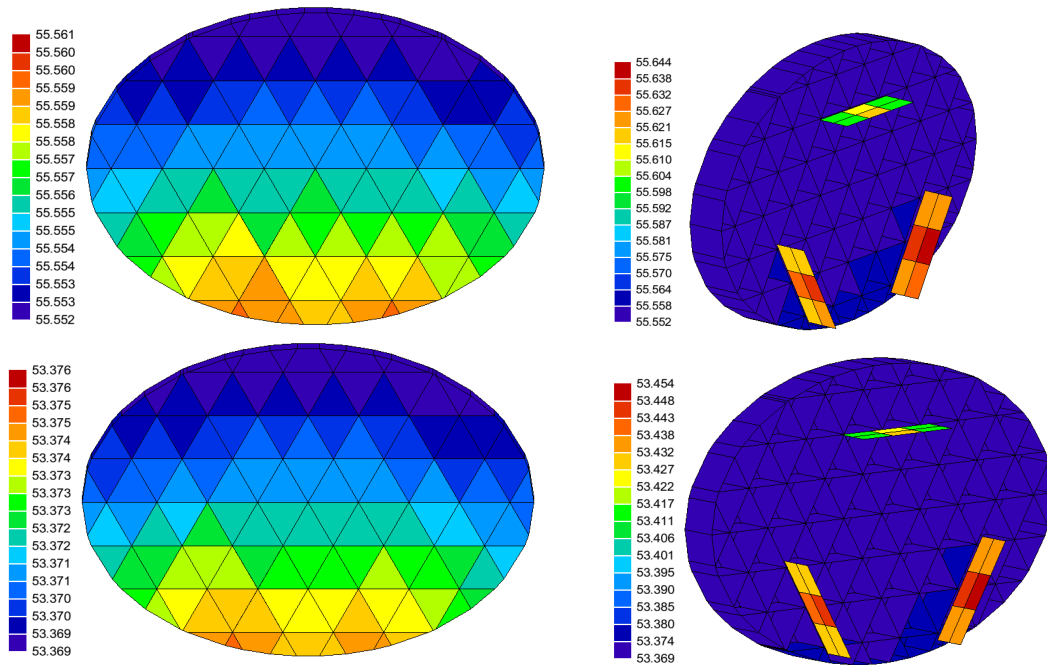


Figure 10. Telescope primary mirror T distribution in the Cold case (lower panels) and the Hot Case (upper panels)

## 5.2 Telescope Assembly GTMM

The TA is a major part of the PLM Geometrical and Thermal Mathematical Model (GTMM). The TA average temperature is around 52.5 K and 55 K respectively in the Cold and Hot Cases (see Fig.9). The 3 K difference between the two extreme cases, when the PLM interfaces temperature differ by nearly 80 K, shows the very high level of insulation from the warm part of the S/C reached with the present PLM/TA thermal architecture.

In the two thermal cases, M1 operates around 53.5 K and 55.5 K with a total gradient across its surface of less than 5 mK, as shown in Fig.10, due to the good thermal uniformity of the mounting interfaces on the TOB and to the good thermal conductance of the mirror itself. The thermal stability of the mirrors is another key issue for the TA performance. Presently, the specification for the max thermal instability at the Spacecraft interface is 10 K over 10 hours.

The worst-case fluctuations are the slowest ones, as they are not filtered out efficiently by the thermal capacitance of the PLM. For this reason, to simulate the effect of this fluctuation level on the mirrors, it is assumed a slow but constant variation of 1K/h over the 10 hours' period and the impact at M1 and M2 level is analysed. The two mirrors show a different behaviour with time. The M1 temperature remains nearly constant, decreasing by a small fraction of a mK, due to the good level of thermal insulation and the high thermal capacitance of the primary mirror. The M2, on the other side, is less insulated from the Telescope Metering Structure, has a lower capacitance and can feel the influence of the shorter front bipod. For these reasons, its temperature change is of the order of 2 mK. In summary, the TA thermal design shows a very high level of insulation and stability for both mirrors. There are still margins to increase the thermal resistance of the M2 from the TMS, if necessary, to further reduce the impact of possible conducted fluctuations.

## 5.3 Thermal Control System

The TA thermal performance is based on a purely passive architecture, part of the general PLM Thermal Control System. The thermal status of the TA is continuously monitored by a set of thermistors controlled by the TCU. The task of this monitoring system is to measure the temperature of some thermal reference points and critical units, as mirrors M2M and TOB, to check their thermal status and health. At present, no need for active thermal control of M1 is expected. However, it is agreed to keep open in the TCU design the option of having an active control of M1 if the need for temperature stabilization of M1 arise because of the STOP analysis. The TA thermal monitoring system is combined with a separated set of thermistors and heaters needed for Decontamination and Survival heating.

# 6. TECHNOLOGY DEVELOPMENT ACTIVITIES

Some technology development activities (TDA) are running during the project phase A and phase B to face and solve the technology risks related to the Ariel telescope aluminum mirrors and the M2 refocusing mechanism (M2M). The mirror M1 has a number of critical technical issues. A TDA program has addressed de-risking of the manufacturing processes, the thermal stability of the large-size aluminum mirror operating at cryogenic temperature and silver coating to raise the TRL of the Al M1 mirror to 6. The conclusion of this activity was that only part of the processes has been qualified; therefore, further activities on two mirror breadboards and two sets of smaller mirror samples are still running. A specific program has addressed de-risking of the M2M operating at 40K instead of 100K, as in the Euclid project. This activity has demonstrated an optimal behavior at the cryogenic operating temperature in terms of design and for all its parts, with the exclusion of the motor-reducer, which failed the duration tests. The plan is to bring these technologies to TRL6 at the Payload PDR (September 2022) with possible minor extension to the TA PDR (Q4 2022).

## 6.1 M1 mirror

Several activities were put in place to raise the TRL of the Ariel M1 mirror. INAF/ASI and ESA activated industrial-technological development activities to reduce the risks associated to the development of the M1 mirror, a large-size cryogenic Al mirror; as such kind of mirrors has never been used in European space missions before Ariel, M1 is considered one of the activities at greatest risk in the Ariel program. Process and manufacturer qualifications have concerned the thermal stabilization of the material, the diamond turning fine figuring and the polishing of the Al optical surface, and the protected-silver coating.

The TDA activity is a two-step process: a first program, called Pathfinder Telescope Mirror (PTM), was based on a M1 prototype, fully representative in size and lightweighting, that underwent all the processes and tests for qualification. The

lesson learnt were applied to a second set of prototype mirrors, two breadboards having circular shape instead of elliptical with diameter 0.7 m. This is for matching the maximum size of the currently available diamond turning machine (LT Ultra Precision, model MT650), since the machine for the larger elliptical mirror is still under development and it will be ready to manufacture the M1 EQM (LT Ultra Precision, model MT1200). Fig. 11 shows the M1 manufacturing flow that is based on a recipe developed at the NASA Goddard Space Flight Center<sup>8</sup> and under development and testing in Italy.

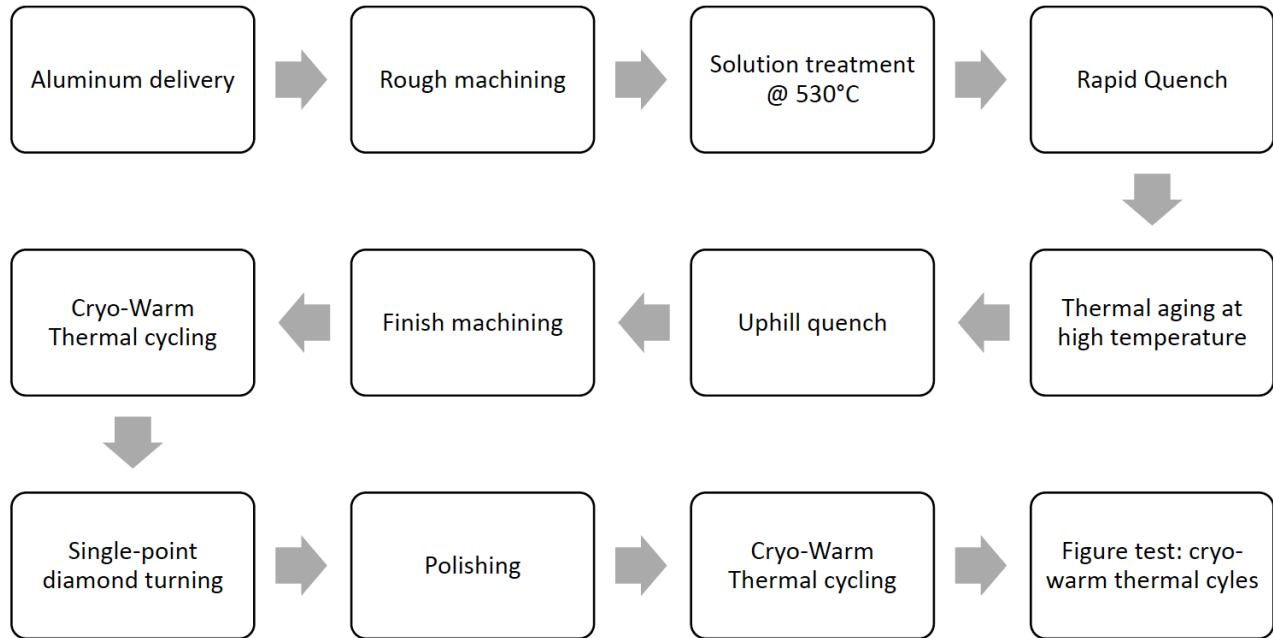


Figure 11. Manufacturing flow of the Ariel telescope mirrors.

The two M1 breadboards will follow different development tasks because there is the need for the Ariel program to obtain a preliminary technology assessment by the Payload PDR (September 2022) that will be completed by the Instrument PDR (January 2023):

- BB#1 will mitigate the risk on the overall manufacturing process and the performance of a large-size Al mirror; it will follow the same manufacturing process as Ariel M1, undergoing an appropriate de-tensioning process through thermal cycles, as reported in Fig.2 and after the lesson learnt on the PTM program
- BB#2 will de-risk the manufacturing processes, i.e., roughing, lightening, diamond turning and polishing.

Some encouraging results have been already achieved:

1. The infrared high-reflectivity protected-silver coating has been qualified and can withstand the warm-cryogenic thermal cycles
2. The diamond turning process provides specifications better than the requirements on the breadboard mirrors
3. The thermal cycling recipe provides a better material in terms of size and distribution of agglomerates and internal stresses; the results on the PTM suggest that the mirror is stable after all the thermal treatments

## 6.2 M2 mechanism

This activity is led by Sener Aerospace (Spain) under the scientific responsibility of IEEC. The M2 mechanism (M2M) is based on the GAIA and EUCLID heritage based on an M2M developed to operate at 100K; it has three linear actuators symmetrically arranged to generate two rotations and one vertical translation. The linear actuator for the Ariel M2M is a

mechanism that provides resolution better than 0.1  $\mu\text{m}$  over a travel of 700  $\mu\text{m}$  with stable position at any point of the stroke. It also has high-load capability to withstand launch loads without back driving.

The different components of the actuator are basically:

- A motor-reducer, which includes a stepper motor and two-stages gear reducer with a M3 thread spindle at output.
- A symmetrical flexible structure, which includes two levers, two flexural joints or pivots, the output interface providing a reduction ratio and the I/F fixed part.
- A nut assembly, which joins the flexible structure via two blades to the spindle.
- Two-ends stops at the beginning and end of the stroke for nut and blades protection and zeroing.
- Two micro-switches one main and one redundant for turns counting.
- One structure supporting both the motor-reducer and the top support of the spindle.

The M2M actuators steppers will be sequentially driven by the Telescope Control Unit electronics. The driver of the stepper shall control the excitation current of each phase to consider the large impedance variations of the coils between ambient and 40K. Although the M2M is at cryogenic temperatures, the electronics will be in the warm section of the spacecraft. This leads to the need of a dedicated cryo-harness able to ensure thermal isolation from the electronics and at the same time good electrical conductivity.

The unit to be manufactured and qualified for the Ariel M2M should be an improved version of the one used in EUCLID. The only modification of the requirements will be the minimum operating temperature, which will be 40K instead of 100K. This is the main reason justifying the technology development. The M2M has demonstrated an optimal behavior at the cryogenic operating temperature in terms of design and for all its parts, with the exclusion of the motor-reducer, which needs further development and testing to improve the mechanism duration.

## ACKNOWLEDGMENTS

This activity has been developed under the Implementation Agreement n. 2021-5-HH.0 "Italian Participation to Ariel mission phase B2/C" between the Italian Space Agency (ASI) and the National Institute for Astrophysics (INAF) and under the ASI contract n. 2021-21-I.0 "ARIEL TA Phase B Industrial Activities" to Leonardo S.p.A and Media Lario s.r.l. companies.

## REFERENCES

- [1] Tinetti, G., et al., "A chemical survey of exoplanets with ARIEL", *Experimental Astronomy* 46, 135–209 (Nov. 2018).
- [2] Da Deppo, V., Middleton, K., Focardi, M., Morgante, G., Claudi, R., Pace, E., and Micela, G., "The optical configuration of the telescope for the ARIEL ESA mission," *Proc. SPIE* 10698, 106984O (2018).
- [3] Rataj, M., Wawer, P., Skup, K., Sobiecki, M., "Design of fine guidance system (FGS) for ARIEL mission," *Proc. SPIE* 11176, 111763E (2019).
- [4] Amiaux, J., Berthé, M., Boulade, O., Cara, C., Lagage, P.O., Moreau, V., Hamm, V., Morinaud, G., Ollivier, M., André, Y., Geoffray, H., Eccleston, P., Middelton, K., Pascale, E., Frericks, M., Focardi, M., Pace, E., EPSC2018-652-1, 12 (2018).
- [5] Ramos Zapata, G., Sánchez Rodríguez, A., Belenguer Dávila, T., Urgoiti E., Ramírez Quintana, A., "Optical tests of a space mechanism under an adverse environment: GAIA secondary mirror mechanism under vacuum and thermal controlled conditions," *Proc. SPIE* 6671, 667117 (2007).
- [6] Artiagoitia, A., Compostizo, C., Rivera, L., *Proc. 'ESMATS 2017'* (2017).
- [7] <https://www.thorlabs.com/>
- [8] Raymond G. Ohl IV, Michael P. Barthelmy, Said Wahid Zewari, Ronald W. Toland, Joseph C. McMann, David F. Puckett, John G. Hagopian, Jason E. Hylan, John Eric Mentzell, Ronald G. Mink, Leroy M. Sparr, Matthew A. Greenhouse, John W. MacKenty, "Comparison of stress-relief procedures for cryogenic aluminum mirrors," *Proc. SPIE* 4822 (2002).